

IDŐJÁRÁS

Quarterly Journal of the Hungarian Meteorological Service
Vol. 126, No. 1, January – March, 2022, pp. 87–108

Spatiotemporal distribution of the climatological fronts over Europe in the modern climate period

Inna Semenova^{1,*} and Katsiaryna Sumak²

¹ *Odessa State Environmental University*
Department of Military Training
15 Lvivska Str., 65016, Odessa, Ukraine

² *Republican center for hydrometeorology,*
control of radioactive contamination
and environmental monitoring (BELHYDROMET)
Department of Meteorological forecasts
110, Nezavisimosti ave, 220114, Minsk, Belarus

**Corresponding author E-mail: in_home@ukr.net*

(Manuscript received in final form December 22, 2020)

Abstract— The geographical position of the Arctic front and two branches of the Polar front over Europe was determined during the period 1995–2015 using calculated grid fields of the thermal frontal parameter in the troposphere layer of 850–700 hPa. It was revealed that the geographical position of climatological fronts changed both in the cold and warm periods of the year in comparison with climate data. The most recent standard reference period of 1961–1990 recommended by WMO (WMO, 2017) was used for comparison. It is shown that in January there was a shift of the northern and southern branches of the Polar front to the north compared to the reference climate period, and in July the convergence of both branches of the Polar front in the middle latitudes was observed. The Arctic front was characterized by a northern location compared to the climate in both January and July. It is revealed that the main areas of frontogenesis in the cold period of the year were the sea surface, namely, the southern regions of the Norwegian Sea, the central part of the Baltic Sea, and the western half of the Mediterranean Sea. In the summer, more active atmospheric fronts were over the continent in the area of the mountain systems such as the south of the Scandinavian mountains, the north of the Alps and Pyrenees, the Urals, and the lower Volga region. The Arctic front intensified over the Barents and Norwegian Seas in all seasons of the year.

Key-words: thermal front parameter, climatological fronts, frontal zones, Polar front, Arctic front, temperature gradients

1. Introduction

The atmospheric front is one of the most complex objects in the atmosphere, which carries important weather-forming and climatic functions. Therefore, the use of methods that allow simulating the complex structure of the front in order to determine its position in space and time is an actual and not completely solved problem.

Objective identification of fronts usually requires 5 subjective choices (*Thomas and Schultz, 2019*): 1) a thermodynamic quantity (e.g., potential temperature, equivalent potential temperature, wind); 2) a mathematical function that operates the value to create a field for identifying the front (e.g., gradient, thermal frontal parameter, frontogenesis); 3) a level or layer where the analysis is performed (e.g., surface, 850 hPa, between 850 and 700 hPa); 4) a minimum threshold or tolerance of the field value for the feature that will be considered a front (e.g., value of the horizontal gradient of a potential temperature exceeding 8K (100 km)^{-1}); 5) an algorithm that allows to draw the front line or identify an area that represents the frontal zone in a field with a specified threshold, and classify the front as warm or cold.

The most common quantitative characteristics of atmospheric fronts are front parameters, which functionally link meteorological values and describe their behavior in the frontal zone, which allows setting some limit criteria specific to the fronts.

As a quantitative characteristic of atmospheric baroclinicity, the front parameter Ψ was proposed by *Huber-Pock and Kress (1989)*, which is a horizontal gradient of the gradient modulus of the equivalent thickness of the *ZTE* (zero thermal expansion) layer enclosed between isobaric surfaces of 925-700 or 850-500 hPa:

$$\Psi = \nabla |\nabla ZTE| \cdot \vec{n}_{ZTE}, \quad (1)$$

where \vec{n}_{ZTE} is a unit vector (normal to the *ZTE* contour line) directed to the area of minimum temperature and humidity values.

The equivalent layer thickness is a function of temperature and humidity on the corresponding isobaric surfaces and, therefore, it is a complex characteristic of air masses:

$$ZTE = - \sum_{P_l}^{P_u} \frac{R}{g} \bar{T}_e \ln \left(\frac{P_u}{P_l} \right), \quad (2)$$

where R is the specific gas constant, g is the acceleration of gravity, u and l are the upper and lower isobaric surfaces, respectively. \bar{T}_e is the function of the equivalent layer thickness bounded by isobaric surfaces P_u and P_l :

$$\bar{T}_e = T + \frac{Lq}{C_p}, \quad (3)$$

where q is the specific humidity, T is the air temperature, L is the specific heat of vaporization, and C_p is the specific heat capacity at constant pressure.

Taking into account the constant values $L = 2.5104 \text{ J}\cdot\text{kg}^{-1}$ and $C_p = 1004.64 \text{ J}\cdot\text{kg}^{-1}\cdot\text{K}^{-1}$, Eq.(3) takes the form for calculating the equivalent temperature:

$$T_e \cong T + 2.5q, \quad (4)$$

where q is expressed in $\text{g}\cdot\text{kg}^{-1}$.

A new approach for expressing the front parameter Ψ was proposed in the studies of Russian scientists (*Shakina et al.*, 1998a,b). Due to the fact that the measure of atmospheric baroclinicity is the number of isobar-isosteric solenoids, which is associated with the horizontal gradient of the layer thickness, the areas where the baroclinicity gradient has a maximum in the direction of the layer thickness gradient should be defined as frontal zones. As a result, the formula for calculating the front parameter Ψ takes the form:

$$\Psi_{ZTE} = \nabla|\nabla ZTE| \cdot \vec{n}_{ZTE}. \quad (5)$$

Since the front line near the ground is located on the warm side of the zone of maximum gradients, it follows from Eq.(5) that only positive Ψ_{ZTE} values can be associated with the front. In order to take into account humidity in the zone of atmospheric fronts *Shakina et al.* (1998b) considered the humidity index, which is expressed by the ratio:

$$HIX = \frac{\nabla ZTE - \nabla ZT}{\nabla ZTES - \nabla ZT}, \quad (6)$$

where the $ZTES - ZTE$ function is calculated for saturated air, ZT is an analogue of the ZTE function calculated by normal temperature.

The humidity index HIX allows identifying zones of atmospheric fronts, where cloud cover and precipitation are observed.

Further, *Shakina et al.* (2000) introduced a dimensionless front parameter F , which is a linear combination of cyclonicity and baroclinicity:

$$F = P + \Psi, \quad (7)$$

where parameter P is a characteristic of cyclonicity and baroclinicity of the lower troposphere (925–850 hPa), and Ψ is the characteristics of baroclinicity in layers 850–500 hPa or 925–700 hPa.

One of the most commonly used parameters in meteorological practice is the thermal front parameter (*TFP*), which is a quantitative characteristic that takes into account the distribution of temperature gradients (*Creswick, 1967; Hewson, 1998; Serreze et al., 2001*).

The thermal front parameter reflects the basic definition of the atmospheric front, namely, on the cold front the temperature begins to decrease, and on the warm front its rise stops. The temperature for calculating the *TFP* can be taken at any level, or calculated in a certain layer of the atmosphere, which allows taking into account the three-dimensionality of the frontal zones. The equivalent temperature T_e is calculated instead of the usual temperature in order to take into account the moisture content. The position of the front line is determined through the zone with the maximum positive values of *TFP* (*Berry et al., 2011a; Hewson, 1998*).

Using the average monthly temperature fields for calculating *TFP* allows identifying baroclinic zones that correspond to the main climatological fronts (*Semenova, 2010*). Moreover, the daily *TFP* fields taking into account humidity can be used to clarify the structure and position of the frontal systems in extratropical cyclones (*Semenova and Ivus, 2011*).

The *TFP* fields are in a good agreement with the cloud zones in satellite images: the bright areas of frontal clouds in the images correspond to the areas of positive *TFP* values. It is shown that the calculated *TFP* fields occupy a certain position relative to the cloud band of the cold front, and these positions remain constant for the next 12 h in most cases, which confirms the need to use numerical *TFP* calculations in operational practice (*Zwatz-Meise and Hufnagl, 1990*).

The method described by *Hewson (1998)* allows calculating several functions from thermodynamic variables to horizontal winds on isobaric surfaces at grid points, which makes it possible not only to identify fronts numerically, but also to determine their type. The same technique was applied in a study by *Berry et al. (2011a)*, which allowed the authors to calculate objective global front climatology using ERA-40 reanalysis data with a spatial resolution of $2.5^\circ \times 2.5^\circ$ for the period 1958–2001. The wet bulb potential temperature fields (Θ_w) at the level of 850 hPa were used to calculate the *TFP*. It was found that in the Northern Hemisphere, the maximum frontal frequency is typical for the North Atlantic and Pacific Oceans, and the highest values are typical for the western parts of these basins. The direction of the fronts here is from southwest to northeast, which is consistent with the trajectories of extratropical cyclones.

The same authors (*Berry et al., 2011b*) expanded their previous research by using four reanalysis datasets such as Era-Interim, NCEP 2, JRA, and MERRA, for studying global trends in objective atmospheric fronts for the period 1989–2009. There was a decrease in the average annual frequency of fronts (by 10–20%) between 30 and 50°N, from the USA to Central Europe. Towards the pole, a local increase was observed near Iceland. In the North Atlantic region, fronts have become less common.

A comparative analysis of two methods of objective identification of fronts in the lower troposphere for different synoptic situations was performed by *Schemm et al.*, 2015. The first method is thermal, based on a gradient of equivalent potential temperature at the level of 850 hPa, the second is based on temporary wind changes at the level of 10 m. It was found that the thermal method allows identifying both cold and warm fronts and quasi-stationary ones, especially in strong baroclinic situations, which include classical extratropical systems of low pressure. The second method is most appropriate for identifying fronts in weak baroclinic synoptic situations, when the frontal systems are induced by strong wind shear and convergence between two anticyclones. The authors also obtained the climatology of fronts for the winter and summer seasons of both hemispheres for the period 1979–2012 according to the Era-Interim reanalysis. The highest frequency of fronts in the Northern Hemisphere in winter was identified in the two main cyclonic regions of the North Atlantic and the Pacific Oceans. Almost complete absence of fronts prevailed over the continental part (Eurasia). In the summer, the maximum of frontal activity shifted northward with a noticeable decrease in frequency. There is an increase in cyclonic activity, especially over the Great Lakes and Hudson Bay, as well as in Western Europe. The orientation of the fronts identified by the thermal method has a more zonal component than the wind one (more meridional orientation of fronts).

Thomas and Schultz (2019) also used gradients of equivalent potential temperature and the wind field to determine the fronts and their location at the surface and 850 hPa during the period 1979–2016. The threshold of $2.0 \text{ K (100 km)}^{-1}$ was chosen as minimum, because it most closely corresponds to the surface analysis of DWD (Deutscher Wetterdienst). It was found that the regions with the highest *TFP* frequency exceeding the threshold value are located near mountain ranges, as well as in lower latitudes, especially over the tropical Eastern Pacific and the Indian Oceans. The *TFP* can not only represent fronts at mid-latitudes, but also represent air mass boundaries from the subtropics, which are largely the result of humidity gradients. Proof of the importance of taking humidity into account in *TFP* calculations is that the mathematical expression for *TFP* includes higher derivatives, and humidity contains much greater variability than temperature, especially in wetter low latitudes. As a result of global averaging, it is revealed that the fronts at the surface are more intense than at the level of 850 hPa. About 10% of the most intense fronts near the surface are more common over land than over the oceans.

The study of *Bitsa et al.* (2019) developed a scheme for identifying cold frontal systems in the Mediterranean basin based on the Frontal Tracking Scheme (FTS), which were developed in the University of Melbourne, Australia. This modified scheme takes into account the particular characteristics of the Mediterranean fronts and includes two criteria – total wind direction change and total wind magnitude for the better identifying of the positions and tilt of a Mediterranean cold front. Thermodynamic criteria were not included in this

scheme, meaning that wind shear is a prerequisite for the transition of the baroclinic zone to an organized cold front in the Mediterranean Sea. A good agreement was obtained between the objective cold fronts and the frequency of the fronts detected as a result of synoptic analysis over Greece.

Catto et al. (2014) estimated future changes (period of 2080–2100) in the frequency of atmospheric fronts using the high emission scenario RCP 8.5. Forecasts showed a decrease in frequency in the Northern Hemisphere, with a shift to the pole of maxima, and a significant decrease in high latitudes, where the temperature gradient decreases. Changes in the frequency of fronts in the future will be strongly associated with changes in the trajectories of cyclones, and these changes are not so clear due to the uncertainty of "their response" to climate warming.

The aim of this study is to determine the spatial and temporal distribution of the climatological frontal zones over Europe in the period of 1995–2015 using the thermal front parameter.

2. Materials and methods

The method of objective analysis of the climatological frontal zones was applied using the calculated grid fields of the thermal front parameter over the European sector, in restricted area 13°W – 62°E and 35–80°N, using the formula (*Creswick, 1967; Hewson, 1998; Serreze et al., 2001*):

$$TFP = -\nabla|\nabla T| \frac{\nabla T}{|\nabla T|}, \quad (8)$$

where $\nabla = \vec{i} \frac{\partial}{\partial x} + \vec{j} \frac{\partial}{\partial y}$ and $|\nabla T| = \sqrt{\left(\frac{\partial T}{\partial x}\right)^2 + \left(\frac{\partial T}{\partial y}\right)^2}$ is the module of temperature gradient.

The initial data for calculating the *TFP* were the daily temperature fields T (K) and specific humidity q ($\text{kg}\cdot\text{kg}^{-1}$) at the 850 and 700 hPa pressure levels of the Era-Interim reanalysis data with a spatial resolution of $1.5^\circ \times 1.5^\circ$ (*ERA Interim, Daily datasets, 2019*).

Eq.(8) includes the equivalent temperature T_e averaged in the layer 850–700 hPa, determined by the formula:

$$T_{e(850-700)} \cong T_{850-700} + 2.5q_{850-700}, \quad (9)$$

where q (specific humidity) is expressed in $\text{g}\cdot\text{kg}^{-1}$.

As the calculated *TFP* fields have the order of magnitude of $10\text{--}11^{-2} \text{K}\cdot\text{m}^{-2}$, in further analysis, we will operate with *TFP* units (without specifying the exponent).

To determine the average monthly position of the frontal zones, the frequency of positive *TFP* values in each point of the calculated grid and the average intensity of the front were analyzed. The latitudinal zone, within which the total number of points with positive values at each latitude was the largest with the simultaneous highest average value of the *TFP*, was taken as the position of the front. At the same time, information on the climatic position of the axes of altitudinal frontal zones was also taken into account (Vorobyov, 1991).

This article presents the results of an objective analysis of climatological fronts for the central months of the seasons and averaged by seasons.

3. Results and discussions

3.1. Geographical position of the frontal zones

The latitudinal zones defined by the described method, as well as the latitudes with maximum parameters that correspond to the average position of the climatological fronts (Arctic front, northern branch of the Polar front (further - NPF), southern branch of the Polar front (further - SPF)) for the central months of the seasons of the studied period are shown in *Table 1* and specified as ‘fact’. Information on the position of climatological fronts was available only in January and July (Khromov and Petrosyants, 2006) for the reference climate period 1961–1990 (WMO, 2017) and provided as ‘climate’ in this table for comparison for the respective months. For April and October, a comparison of the geographical position of the fronts was performed only in comparison with the previous season within the study period.

Table 1. Geographical latitudes of the position of the frontal zones (°N) for the period 1995–2015 (fact) and according to climate data (climate)

Month	NPF		The interval of latitudes (fact)	SPF		The interval of latitudes	Arctic		The interval of latitudes (fact)
	fact	climate	(fact)	fact	climate		fact	climate	(fact)
January	59.0	56.0	57.5-59.0	42.5	39.3	41.0-44.0	72.5	68.3	69.5-74.0
April	60.5	-	59.0-60.5	51.5	-	50.0-53.0	75.5	-	74.0-75.5
July	62.0	64.2	60.5-66.5	51.5	47.9	48.5-53.0	77.0	73.0	75.5-77.0
October	62.0	-	62.0-65.0	42.5	-	41.0-44.0	69.5	-	69.5-72.5

As seen, the position of the northern and southern branches of the Polar front in winter (January) has changed compared to the climate data, namely, there was a shift to the north by three degrees of latitude of both branches. In the summer

period (July), the northern branch, on the contrary, occupies a more southerly position compared to the previous period, and the southern branch has shifted to the north by more than three degrees of latitude. In the spring (April), the northern branch occupies an intermediate position between the winter and summer periods, while the southern branch is characterized by the greatest shift to the north (by 9 degrees of latitude) in comparison with the winter period, and thus, its position in April and July is identical. In the autumn (October), the northern branch did not change its position relative to the summer location, while the southern branch shifted south by almost 11 degrees of latitude.

The position of the Arctic front in the cold and warm periods of the year also changed in comparison with the previous climate period: it shifted to the north by four degrees of latitude. In April, there was a significant shift of the front to the northern latitudes in comparison with the cold period of the year, and in October, the Arctic front occupies its highest position among the considered months at longitude 69.5°N.

3.2. Spatiotemporal dynamics of frontal zones

The spatiotemporal cross sections of *TFP* fields were constructed as the Hovmöller diagrams for the identified latitudes corresponded to location of main climatological fronts, to determine the time dynamics of the intensity of the frontal zones during the study period.

In *Figs. 1–4*, the distribution of the thermal front parameter at fixed latitudes (which correspond to the described climatological fronts) for central months of the seasons is shown. At all latitudes, areas can be seen with longitudes and time intervals where the fronts are well expressed in the *TFP* fields.

January. The Arctic front is most pronounced over the areas of the Barents Sea and the eastern part of the Norwegian Sea (11–35°E). However, the position of the maximum *TFP* changes over the years (*Fig. 1a*). Thus, the most intense section of the front was located in the longitude range of 11–19°E in 1997, 1999, and in the period 2002–2007, and over the central regions of the Barents Sea – from 2005 to 2009. At the beginning of the study period (1995–1996), the front also intensified (up to 3–5 *TFP* units) in the area of the Jan Mayen Island, which is located to east of Greenland. In the last five-year period, the Arctic front was weakly expressed over the entire longitude interval.

Fig. 1b shows that the northern branch of the Polar front (NPF) in January is the most intense over the southern regions of the Norwegian Sea (13° W-5°E), however, in different years, the position of the maximum *TFP* (up to 3–4 units) in this area changes. Thus, the highest intensity of this section of the front was observed in 1996–1997, 2001–2002, and 2006, as well as in the western part of the region in 2009 and in the eastern part in 2014. Further to the east, the intensity of the NPF decreases significantly, but it is possible to distinguish periods when the front intensified. The front's intensification (up to 1–2 *TFP* units) occurred at

longitudes of 20–33°E, i.e., over the areas of the central part of the Baltic Sea and the Gulf of Finland in the period from 1996 to 1998, as well as in 2006, 2008, and 2011–2012. The front was most intense in the Volga and Ural regions in 1998, 2001, 2003–2004, and 2012–2013. In general, it should be noted that over the sea surface no significant changes in the intensity of NPF were observed during the study period, and over the continental part the front was weaker than over the sea in almost all years.

The distribution of *TFP* at the latitude of the southern branch of the Polar front (SPF) is complex due to the alternation of sea and continental surfaces over longitudes (*Fig. 1c*). In almost all years, the front is well defined from 13°W to 19°E, which corresponds to the area of the Atlantic and the adjacent western half of the Mediterranean Seas. The most intense SPF in this region was in the periods from 2000 to 2006 and from 2009 to 2015, as well as in 1995, when the maximum *TFP* reached 2–3 units of *TFP*.

Further to the east, in the interval of longitude 28–44°E, i.e., over the mountainous areas of the northern part of the Peninsula of Asia Minor and the Lesser Caucasus, the front also intensified from 1995 to 1999 and in the period 2002–2015, and the maximum *TFP* also reached 2–3 units of *TFP*. Thus, in January, during the study period, there was an increase in the intensity of SPF in almost the entire region.

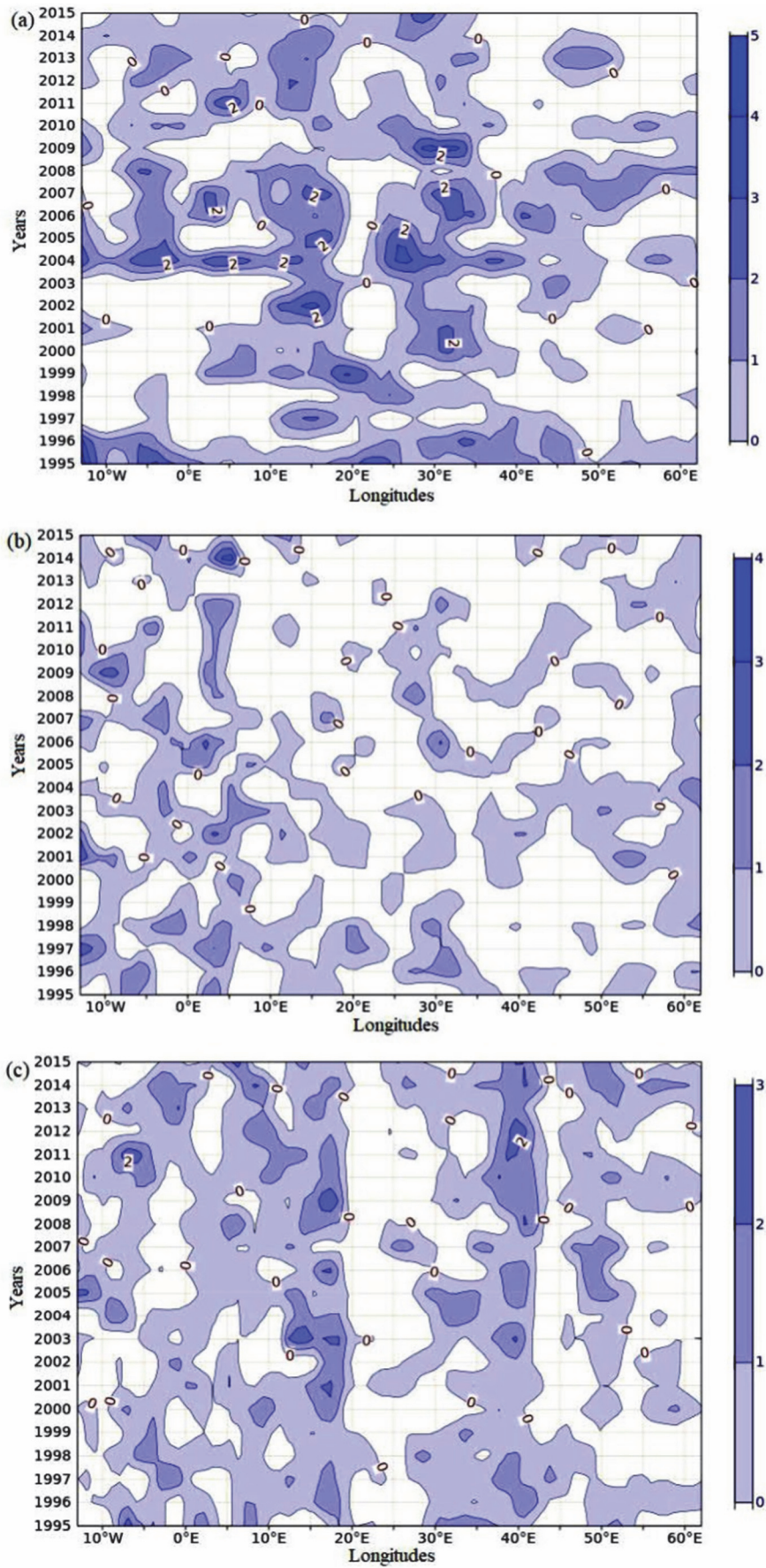


Fig. 1. Spatiotemporal distribution of TFP in January 1995–2015 at latitudes: a) 72.5°N (Arctic front); b) 59°N (NPF); c) 42.5°N (SPF).

April. The Arctic front is most intense over the northern areas of the Norwegian Sea (13°W - 8°E), but in different years the position of the maximum *TFP* (up to 4–5 units of *TFP*) in this area changes. Thus, the highest intensity of this section of the front was observed from 2002 to 2006, as well as in 2015 in the western part of the region, and in 2011 in the eastern part. In 2002–2004 and 2006, the Arctic front was well defined not only over the Norwegian Sea, but also over the Barents Sea (20 – 45°E). The Arctic front also intensified over the western part of the Barents Sea in 2011. As it can be seen from *Fig. 2a*, in general, the Arctic front is weakly expressed, and its intensity in some areas decreases from west to east.

The distribution of *TFP* at the latitude of the northern branch of the Polar front is complex due to the predominance of the continental surface along this latitude (*Fig. 2b*). In almost all years, the NPF front section is well defined in the longitude range from 13°W to 10°E , which corresponds to the southern part of the Norwegian Sea and the south of the Scandinavian Peninsula. In this area, the front was most intense in 1999–2000, 2003–2004, and 2007–2011, when *TFP* values reached 3 units. Further to the east, the intensity of the NPF generally decreases, but it is possible to distinguish periods when the front intensified. In the period 1995–2001, the intensification of the front (up to 3–4 *TFP* units) occurred at longitudes 22 – 33°E , i.e., over the areas of the central part of the Baltic Sea. From 1999 to 2002, the most intense section of the NPF (3–4 *TFP* units) was located within 41 – 56°E , above the continental surface of the Non-Black Earth Region of Russia, and this section of the front was shifted even further to the east in 2005. In general, it should be noted that over the continental surface, there was a decrease in the intensity of NPF during the study period, while in the west, over the sea surface, no significant changes were observed.

The SPF in April was more intense over the continental surface, at longitudes 5 – 38°E . The position of the maximum *TFP* (up to 2–3 units of *TFP*) changes at different times. Thus, in the period 1999–2001, the front intensified over the central regions of Eastern Europe and the Black Earth Region of Russia, and from 2005 to 2009, the most intense section of the front passed over Central Europe (2–3 *TFP* units). At the end of the study period (2012–2015), the intensification of the front was observed at longitudes 8 – 15°E , 32 – 35°E , and the most intense section (up to 4 *TFP* units) was located over the Southern Urals (54 – 62°E). In general, as it can be seen from *Fig. 2c*, the southern branch of the Polar front in April is weakly expressed, especially over the sea surface.

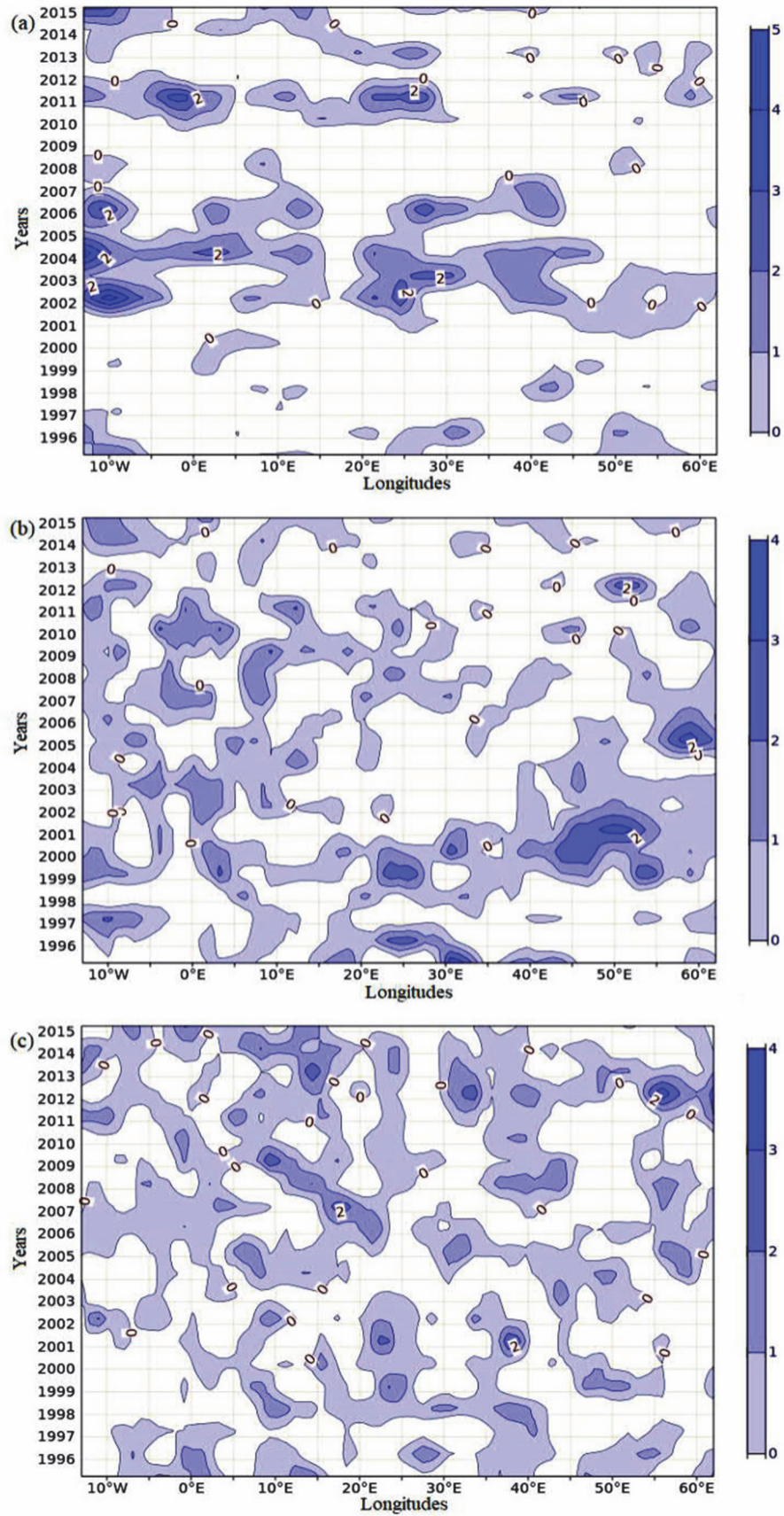


Fig. 2. Spatiotemporal distribution of *TFP* in April 1995–2015 at latitudes: a) 75.5°N (Arctic front); b) 60.5°N (NPF); c) 51.5°N (SPF).

July. In summer, the Arctic front is the most intense (up to 3–5 *TFP* units) in almost all years over the areas of Svalbard Island and the northwestern part of the Barents Sea (15–40°E), and only in the last five-year period this section of the front was weakly expressed. The highest intensity of the front (up to 2–3 units of *TFP*) over the northern part of the Greenland Sea was observed from 1995 to 1997, as well as from 2001 to 2007 and in 2011. In the eastern part of the study region at longitudes 45–62°E, the front intensified from 1997 to 2002, in 2005–2008 and 2012–2015. In general, as it can be seen from *Fig. 3a*, in July the Arctic front was well expressed in certain sections along the longitudes, and no significant changes in its intensity were observed during the study period.

The NPF branch in summer is most intense over the southern regions of the Scandinavian mountains (6–12°E), here in almost all years the maximum *TFP* reached 6–7 *TFP* units (*Fig. 3b*). Over the sea surfaces, i.e., over the southern part of the Norwegian Sea (13°W–5°E) and the central part of the Baltic Sea (18–22°E), the front is less intense. Further to the east, over the continental surface, in general, the intensity of NPF is low, but it is possible to distinguish periods of the highest intensification of the front. Thus, from 1999 to 2001, the front intensified (up to 6–7 *TFP* units) at longitudes of 35–60°E, i.e., over the northeast of the European part of Russia, the Volga region, and the Middle Urals. In 2010–2013, this was also the most intensive section of the NPF (3–6 *TFP* units).

As in winter, the SPF branch is well expressed at almost all longitudes (*Fig. 3c*). The front was most intense (up to 3–5 *TFP* units) in 2006 and 2015 within 6–14°E, which refers to the region of Western Europe, as well as from 27 to 36°E, i.e., over the central part of Eastern Europe and the Black Earth of Russia in 1999 and 2007. Over the Atlantic (13–9°W), the front intensified from 2010 to 2014, when the values of the *TFP* reached 3 units. In the eastern part of the region (44–62°E), the front was most intense (up to 2–3 *TFP* units) in 1997, 2000, 2005, and 2010. In general, there were no trends in changes in the intensity of SPF in summer during the study period.

October. As it can be seen from *Fig. 4a*, in general, the Arctic front is relatively weak, but it is possible to distinguish periods and areas when the front was intensified. Thus, over the northwestern part of the Norwegian Sea (13°W – 0°), the front was well-defined (up to 4–5 *TFP* units) in 2002 and 2005. Over the northern part of the Scandinavian Peninsula, the highest intensity of the front (up to 2–4 *TFP* units) was observed in 2005, 2011, and 2013. Further to the east, over the southern part of the Barents Sea (35–62°E), the intensity of the Arctic front decreases sharply. It can be noted that no changes in the intensity of the Arctic front were detected during the study period.

The northern branch of the Polar front in October occupies the same position as in July (62°N, see *Table 1*), but it has become less intense. From 1995 to 2007, the front is expressed in almost all longitudes. The most intense areas were located over the sea surfaces during this period: over the southern regions of the Norwegian Sea (13°W – 0°), when the maximum *TFP* reached 3–5 units, as well as over the central part of the Baltic Sea and the Gulf of Finland (18–27°E).

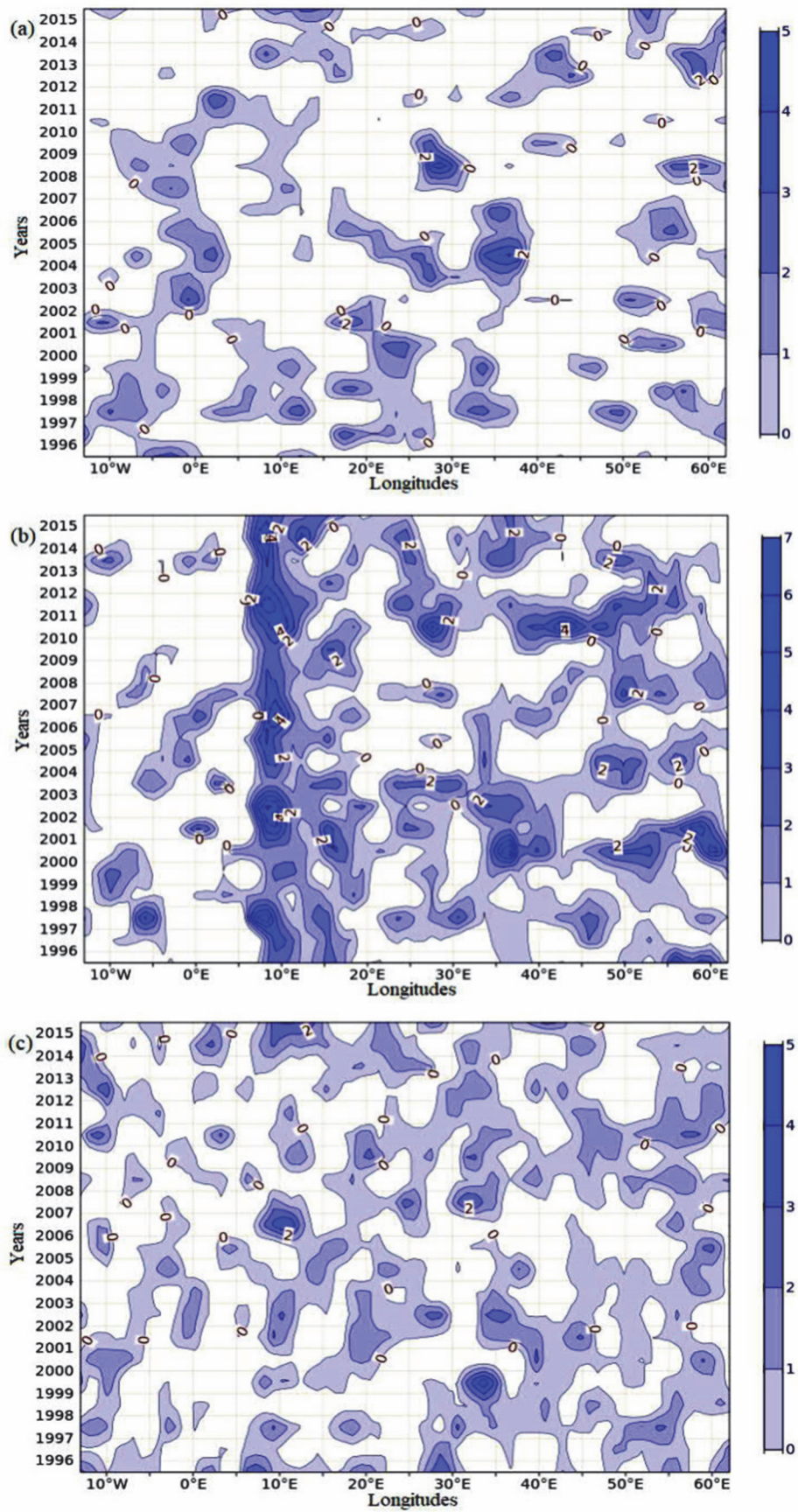


Fig. 3. Spatiotemporal distribution of TFP in July 1995–2015 at latitudes: a) 77°N (Arctic); b) 62°N (NPF); c) 51.5°N (SPF).

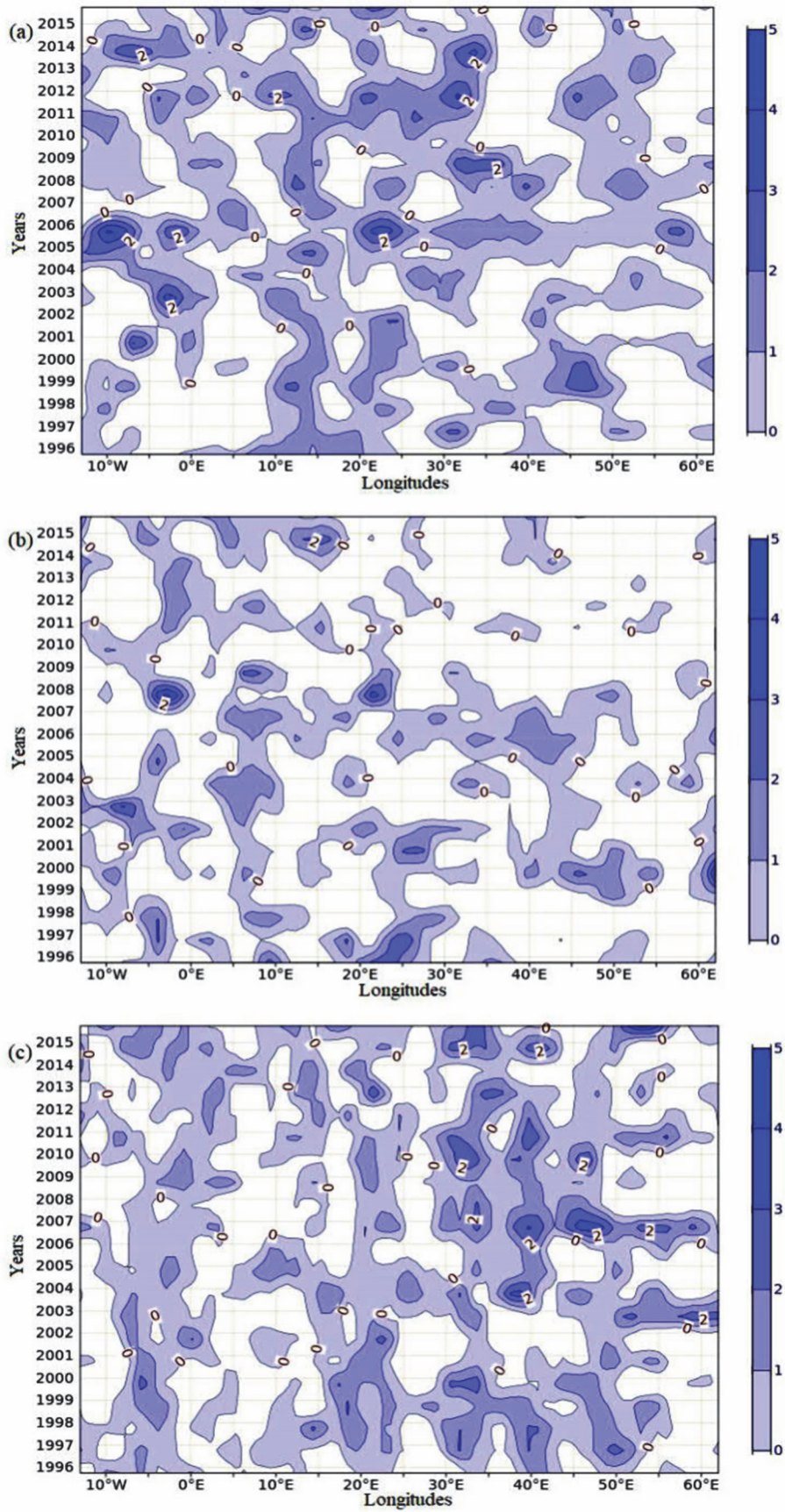


Fig. 4. Spatiotemporal distribution of TFP in October 1995–2015 at latitudes: a) 69.5°N (Arctic front); b) 62°N (NPF); c) 41°N (SPF).

The southern part of the Scandinavian mountains, in the interval of longitude 5–10°E, also turned out to be the area of intensification of the front (2–3 units of TFP). Over the continental surface (30–62°E) in general, the intensity of this section of the front weakens, but there are certain periods of intensification of the front. Thus, the highest activity of the front (2–3 units of TFP) was observed from 1998 to 2000 in the interval of longitude 39–62°E, which corresponds to the regions of the northeast of the European territory of Russia and the Pre-Urals. It should be noted that the intensity of NPF decreased during the study period (*Fig. 4 b*).

As it can be seen from *Fig. 4c*, the SPF branch is most intense over the mountainous areas of the northern part of the Asia Minor Peninsula and the Lesser Caucasus (28–48°E), but the position of the maximum TFP (up to 3–4 TFP units) changes in this area. Thus, the highest intensity of this section of the front was observed from 2003 to 2006, as well as in 2015. Over the Iberian, Balkan, and Apennines peninsulas, as well as the Mediterranean Sea, the front was almost not pronounced, in some years its intensity did not exceed 1–2 TFP units. In general, the southern branch of the polar front is relatively weak in October, and no noticeable trends in its intensity were observed during the study period.

3.3. Seasonal spatial distribution of frontal zones

The geographical distribution of frontal zones over Europe was averaged by season. *Figs. 5–8* show that in all seasons, certain geographical areas are distinguished, where the frontal zones are most intense in the TFP values.

Winter. In winter, within the study region, such zones of active frontogenesis are detected (*Fig. 5*). In the northwestern part, in the latitudes 72–80°N, an area located to the north-east of Greenland with maximum TFP of up to 1–2 units is distinguished, which is justified by baroclinicity conditions due to few factors: contrasts between the warm North Atlantic current and the cold East Greenland current, as well as the Arctic basin located to the north, filled with cold air. Over the Atlantic, the baroclinic zones associated with the Icelandic low are oriented in the meridian direction and take a latitudinal position over Arctic waters along the northern edge of the continent, which coincides with the average trajectories of extratropical cyclones and corresponds to sections of the Arctic front, which is constantly intensifying in this band.

The next zone of seasonal frontal activity extends from the British Isles through the North Sea and adjacent waters along the Scandinavian Peninsula. The maximum TFP (up to 1–2 TFP units) is located in the latitude band 63–69°N near the meridian 10°E, which corresponds to the transition zone between various underlying surfaces as cold land - warm ocean. Atmospheric fronts, approaching the Scandinavian mountains, slow down and intensify, undergoing orographic frontogenesis on the windward slopes.

Over most of the mainland Europe, frontal activity is low, due to the influence of anticyclonic formations, which have a high frequency in the winter season (*Semenova and Najmudinova, 2019*).

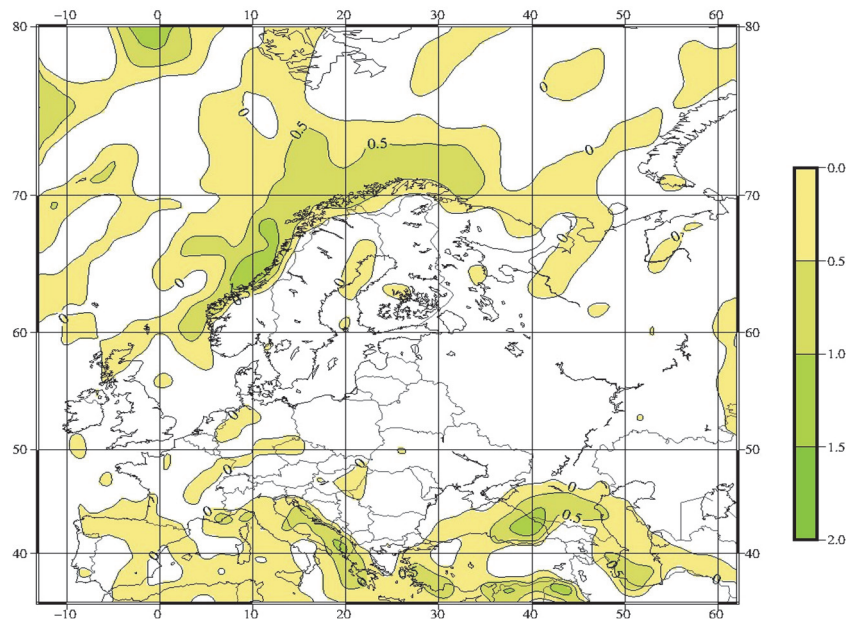


Fig. 5. Average *TFP* field in the winter (December-February) for the period 1995–2015.

Over the territory of Eastern Europe, in the north of the Eastern European plain, a weakened section of the front is revealed, which, according to *Zolotokrylin et al. (2014)*, should be attributed to the secondary branch of the Arctic (subarctic) front, formed as a result of the branching of the main branch of the Arctic front over Scandinavia.

In the southern part of Europe, there is an extensive zone of frontal activity, which corresponds to the southern (Mediterranean) branch of the Polar front, which intensifies during the cold season and separates polar and subtropical air masses. The most intense areas of the fronts are over the Gulf of Genoa, the Adriatic Sea, the Eastern Mediterranean, as well as the southeastern part of the Black Sea and the Greater Caucasus mountain system with maximum *TFP* of 1–2 units.

Spring. Compared to the winter period, during the transition season, there is a significant weakening of frontal activity in northern latitudes, which is detected by a significant decrease in the area of zones of positive *TFP* values (*Fig. 6*). However, several of the most intense sections of the fronts can be identified here. As in winter, this is the area to the northeast of Greenland, corresponding to the

section of the Arctic front. The second section of the branch is less intense than in the previous season (the maximum *TFP* does not exceed 1 unit), there is no continuous zone of positive *TFP* values to the east of the Icelandic low, and only small areas are allocated near the northern part of the Scandinavian and Kola peninsulas, as well as the adjacent Arctic basin. It is characteristic that the frontal zones do not spread further to the east along 70°N.

In the spring, high frontal activity persists over the British Isles. The intensity of fronts is weak over areas of Central and Eastern Europe.

The southern (Mediterranean) branch of the Polar front remains acute, and the zone of positive *TFP* values covers a significant area in the southern part of this region. Thus, the maximum *TFP* reaches 1–2 units over the areas of the Iberian Peninsula, the Atlas mountain systems, the Alps, the Greater Caucasus, Zagros, the Armenian highlands, the Carpathians, and the peninsulas of Asia Minor. However, there are almost no fronts over the Mediterranean basin.

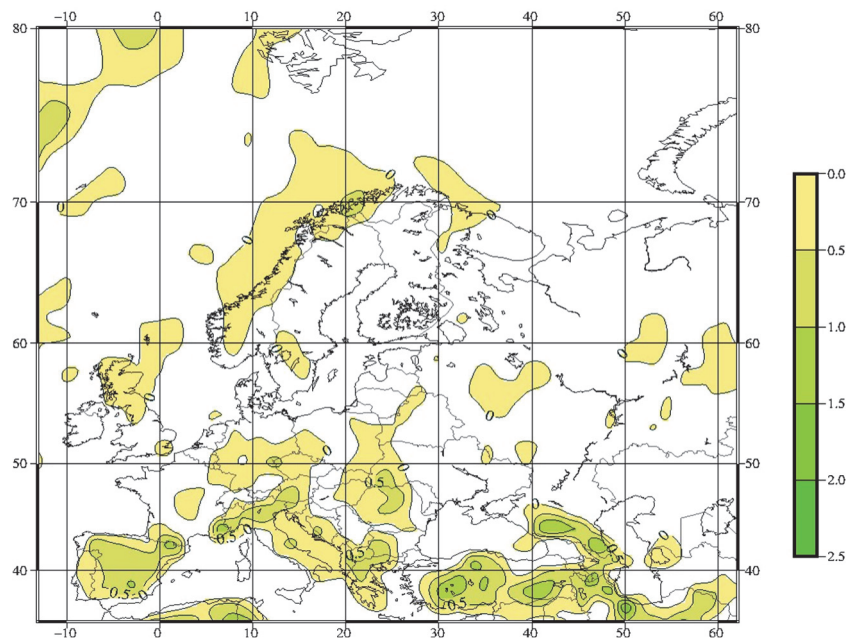


Fig. 6. Average *TFP* field in the spring (March-May) for the period 1995–2015.

Summer. In the summer, in northern latitudes, almost complete absence of frontal zones over the seas is observed, and only a weak section of the Arctic front is fixed over the Greenland Sea (Fig. 7). However, over the mainland, there is a significant intensification of the branches of the Polar front compared to the previous season, including the territory of Eastern Europe. As seen, the baroclinic zone is most clearly manifested in the regions with mountain systems, due to the local increase of the horizontal temperature gradients in the lower troposphere induced by the orographic impact under the general weakening advective processes that is typical for the summertime (Semenova and Najmudinova, 2019).

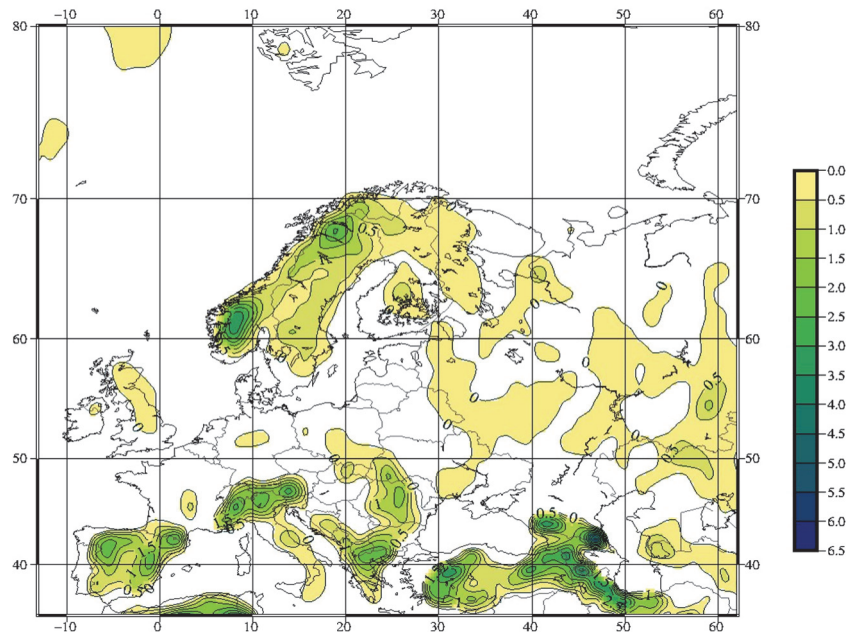


Fig. 7. Average *TFP* field in the summer (June-August) for the period 1995–2015.

The increased activity of fronts over the East European plain is also explained by the predominance of the low pressure field over the warmed continent in the summer season, which contributes to the formation of convergence zones in the lower layers of the troposphere, in which atmospheric fronts can sharpen. The most intense sections of the NPF branch are located above the Scandinavian mountains, with maximum *TFP* up to 3 units.

The southern (Mediterranean) branch of the Polar front is characterized by significant intensity over the land surface. The baroclinic zones (up to 1–3 *TFP* units) located over the Pyrenees, Alps, Carpathians, Atlas Mountains, as well as over the mountain ranges on the Balkan Peninsula and the Asia Minor Peninsula. The intensity of the baroclinic zone reaches 3–7 *TFP* units in the mountains of the Greater and Lesser Caucasus.

Autumn. In the autumn period, the geographical distribution of frontal activity in the study region almost coincides with the spring processes, and in comparison with the summer, there is a significant decrease in the intensity of *TFP* in the frontal sections over the continent (Fig. 8). Zones of positive *TFP* values (maximum up to 1 *TFP* unit) appear again over the waters of the seas in northern latitudes. As in previous seasons, the southern (Mediterranean) branch of the Polar front is distinguished, while the intensity of the maximum *TFP* decreases and does not exceed 1–2 units over the Iberian and Balkan peninsulas, Asia Minor, the mountain systems of the Alps, the Carpathians, and the Atlas. Over the territory of Eastern Europe, the activity of atmospheric fronts is low, which is associated with an increase in the frequency of anticyclonic formations over the continent in this season of the year.

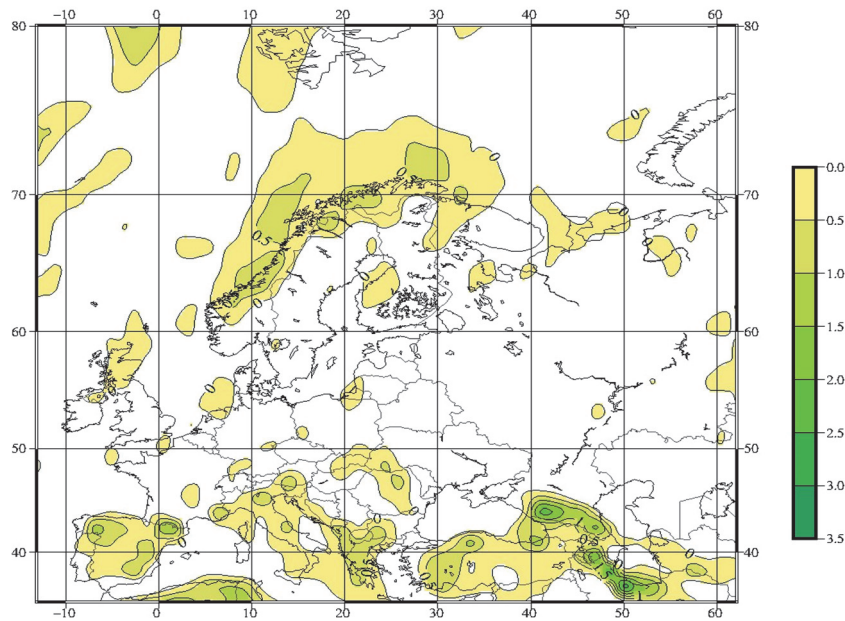


Fig. 8. Average *TFP* field in the autumn (September–November) for the period 1995–2015.

4. Conclusions

The average monthly position of the Arctic front and two branches of the Polar front over Europe in the modern period was established using the calculated fields of the thermal front parameter (*TFP*) in the layer 850–700 hPa. It is revealed that the geographical position of climatological fronts has changed in both the cold and warm periods of the year compared to the climate data. So, in January, both branches of the Polar front shifted to the north by three degrees of latitude. In July, the northern branch of the Polar front descended to the south, the southern branch took a more northerly position, which led to the convergence of the two branches of the Polar front in the middle latitudes. In spring (April), compared to winter, there was a northward shift of the two branches of the Polar front, while in autumn (October), the northern branch did not change its summer position, and the southern branch had the southernmost location during the year. The Arctic front was characterized by northerly location in both January and July compared to the climatic one. In April, a significant shift of the front to the northern latitudes was revealed compared to January, and from mid-autumn to January, the Arctic front occupied the southernmost position among the months of the year. Since cyclonic activity is directly related to atmospheric fronts, the detected front shifts indicate changes in regional synoptic processes over the European continent over the past 20 years, which were reflected in the climate regime of these territories (*Pachauri and Meyer, 2014*).

The main areas of intensification of the branches of the Polar front in the cold period of the year was the southern areas of the Norwegian Sea, central part of the Baltic Sea, the western half of the Mediterranean Sea, the Volga region,

and the mountain ranges of the Urals and Lesser Caucasus. In summer, these were the southern regions of the Scandinavian mountains, the northeast of the European territory of Russia, the Volga region, the Middle Urals, and the mountainous regions of Western Europe. In the spring and autumn, the most intense sections of the front were typical for the southern part of the Norwegian Sea and central part of the Baltic sea, the southern Urals, Central Europe, as well as for the mountainous regions of the northern part of the Asia Minor Peninsula and the Lesser Caucasus. The Arctic front in all seasons of the year intensified over the areas of the Barents and Norwegian Seas, in the summer over the north of the Greenland Sea, and in the autumn also over the northern part of the Scandinavian Peninsula.

In the seasonal distribution, the main zones of frontogenesis in the winter were the territories from the British Isles to the Scandinavian Peninsula, as well as the Gulf of Genoa, the Adriatic Sea, the Eastern Mediterranean, the southeastern part of the Black Sea, and the Caucasus mountain system. During the transition seasons, the most intense sections of fronts were typical for the southern part of the study region, namely, the Iberian Peninsula, mountain systems of Western Europe, North Africa, the Greater Caucasus, and the Asia Minor Peninsula. In the summer season, the intensification of fronts was detected over the continent, with intense baroclinic zones associated with mountain systems such as the Scandinavian mountains, Pyrenees, Alps, Carpathians, Atlas Mountains, the Caucasus. These *TFP* maxima, as shown in other studies (e.g., *Berry et al.*, 2011a), correspond to features of stable baroclinic zones connected with a change in the underlying or/and sloping land surface, but they are not atmospheric fronts in the classical sense (e.g., *AMS glossary*, 2012), although in some cases they can induce local cyclogenesis.

References

- AMS Glossary of Meteorology*, 2012: Available online: <https://glossary.ametsoc.org/wiki/Front>
- Berry, G., Reeder, M.J., and Jacob, Ch.*, 2011a: A global climatology of atmospheric fronts, *Geoph. Res. Let.* 38. <https://doi.org/10.1029/2010GL046451>
- Berry, G., Jakob, C., and Reeder, M.*, 2011b: Recent global trends in atmospheric fronts, *Geoph. Res. Let.* 38. <https://doi.org/10.1029/2011GL049481>
- Bitsa, E., Flocas, H., Kouroutzoglou, J., Hatzaki, M., Rudeva, I., and Simmonds, I.*, 2019: Development of a Front Identification Scheme for Compiling a Cold Front Climatology of the Mediterranean. *Climate* 7(11), 130. <https://doi.org/10.3390/cli7110130>
- Catto, J.L., Nicholls, N., Jakob, C., and Shelton, K.L.*, 2014: Atmospheric fronts in current and future climates. *Geoph. Res. Let.* 41. <https://doi.org/10.1002/2014GL061943>
- Creswick, W.S.*, 1967: Experiments in objective frontal contour analysis, *J. Appl. Meteor.* 6, 774–781. [https://doi.org/10.1175/1520-0450\(1967\)006<0774:EIOFCA>2.0.CO;2](https://doi.org/10.1175/1520-0450(1967)006<0774:EIOFCA>2.0.CO;2)
- ERA Interim, Daily datasets*. 2019: Available online: <https://apps.ecmwf.int/datasets/data/interim-full-daily/levtype=pl/> .
- Hewson, T.D.*, 1998: Objective fronts, *Meteorol. Appl.* 5, 37–65. <https://doi.org/10.1017/S1350482798000553>

- Huber-Pock, F. and Kress, Ch., 1989: An operational model of objective frontal analysis based on ECMWF products. *Meteorol. Atmos. Phys.* 40, 170–180. <https://doi.org/10.1007/BF01032457>
- Khromov, S.P. and Petrosyants M.A., 2006: Метеорология и климатология: учебник. Москва, Изд-во Моск. ун-та, Наука, 582 с. (In Russian)
- Pachauri, R.K. and Meyer, L.A. (eds.), 2014: IPCC. Climate Change 2014: Synthesis Report. Contribution of Working Groups I, II and III to the Fifth Assessment Report of the Intergovernmental Panel on Climate Change. Available online: <https://www.ipcc.ch/report/ar5/syr/>
- Schemm, S., Rudeva, I., and Simmonds, I., 2015: Extratropical fronts in the lower troposphere – global perspectives obtained from two automated methods, *Quart. J. Roy. Meteorol. Soc.* 141, 1686–1698. <https://doi.org/10.1002/qj.2471>
- Semenova, I.G., 2010: Об'єктивний аналіз кліматологічних фронтів в Атлантико-Європейському секторі. *Причорноморський екологічний бюлетень* 2 (36), 47-51. (In Ukrainian)
- Semenova, I.G. and Ivus, G.P., 2011: Использование термического фронтального параметра для моделирования бароклинных зон в процессах циклогенеза. *Наукові праці УкрНДГМІ*, 261, 56-71. (In Ukrainian)
- Semenova, I.G. and Najmudinova, O.M., 2019: Регіональна синоптика: підручник. Одеса: ТЕС, 212 с. (In Ukrainian)
- Serreze, M.C., Lynch, A.H., and Clark, M.P., 2001: The arctic frontal zone as seen in the NCEP-NCAR reanalysis. *J. Climate*, 14, 1550–1567. [https://doi.org/10.1175/1520-0442\(2001\)014<1550:TAFZAS>2.0.CO;2](https://doi.org/10.1175/1520-0442(2001)014<1550:TAFZAS>2.0.CO;2)
- Shakina, N.P., Kalugina, G.Yu., Skriptunova, E.N., and Ivanova, A.R., 1998a: Суб'єктивний и об'єктивний анализы атмосферных фронтов. I. Об'єктивные характеристики фронтов, проведенных синоптиками. *Метеорология и гидрология*, 7, 19-30. (in Russian).
- Shakina, N.P., Skriptunova, E.N., Ivanova, A.R., and Kalugina, G.Yu., 1998b: Суб'єктивний и об'єктивний анализы атмосферных фронтов. II. Об'єктивное выделение зон фронтов. *Метеорология и гидрология*, 8, 5-15. (in Russian).
- Shakina, N.P., Skriptunova, E.N., and Ivanova, A.R., 2000: Об'єктивний аналіз атмосферних фронтів и оцінка його ефективності. *Метеорология и гидрология*, 7, 5-16. (in Russian).
- Thomas, C.M. and Schultz, D.M., 2019: Global Climatologies of Fronts, Airmass Boundaries, and Airstream Boundaries: Why the Definition of “Front” Matters, *Month. Weather Rev.* 147, 691–717. <https://doi.org/10.1175/MWR-D-18-0289.1>
- Vorobyov, V.I., 1991: Синоптическая метеорология. Ленинград: Гидрометеиздат. 616 с. (In Russian)
- WMO, 2017: Guidelines on the Calculation of Climate Normals. WMO Publisher No. 1203. Geneva. Available online: https://library.wmo.int/doc_num.php?explnum_id=4166
- Zolotokrylin, A.N., Titkova, T.B., and Mikhailov, A.Yu., 2014: Климатические вариации арктического фронта и ледовитости Баренцева моря. *Лёд и Снег*, 1 (125), 80-85. (In Russian) <https://doi.org/10.15356/2076-6734-2014-1-85-90>
- Zwatz-Meise, V. and Hufnagl, F., 1990: Some results about the relation between an objective front parameter and cloud bands in satellite images and its connection to classical cold front models, *Meteorol. Atmos. Phys.* 42, 77–89. <https://doi.org/10.1007/BF01030580>